CEAI, Vol.26, No.3, pp. 32-40, 2024 Printed in Romania

Online Propeller Fault Detection with Variable Sliding Window and Adjustable Gain under Variable Velocity and Current Conditions

Wenxia Zhang*, Jian Yuan[1], Song Ge**, Hailin Liu****

** Department of Mechanical and Electrical Engineering, Qingdao Institute of Technology, Qingdao, China (e-mail: dasinusheng@163.com)*
*** Institute of Oceanographic Instrumentation, Qilu University of Technology (Shandong Academy of Sciences), Shandong Provincial Key Laboratory of Ocean Environment Monitoring Technology, National Engineering and Technological Research Center of Marine Monitoring Equipment, Qingdao, China; Key Laboratory of Ocean Observation Technology, MNR, Tianjin, China (e-mail: yuanjian@qlu.edu.cn)*
[1]Corresponding Author: Jian Yuan

Abstract: Neural networks and deep learning for fault diagnosis requires a significant amount of data to train the network model. Continuous parameter tuning is essential. Despite employing regularization techniques to improve the algorithm's performance on the training set, it lacks strong generalization capabilities for fault detection in the variable operating conditions of underwater thrusters. Additionally, the algorithm exhibits high computational complexity, leading to suboptimal real-time fault detection and limited adaptability. To address real-time detection in the case of entanglement, the correlation analysis method with variable sliding window is proposed, a kind of online adjustable gain fuzzy clustering method is carried out to deal with the entanglement detection. The electrical current and velocity collecting application is designed to gather electrical current and velocity from submerged propellers in various operating states using the variable sliding window method, and then standardize the gathered information. The correlation matrix is used to detail the cross-correlation and autocorrelation between standardized sensors data using a sliding window for data-collecting series. An adjustable gain fuzzy clustering method with improved distance index is used to detect the entanglement based on the correlation matrix elements. During the process of real-time correlation analysis and entanglement detection, the variable sliding window method is used for capturing accurately of variant electrical current and velocity information. The adjustable gain is adopted in the fuzzy clustering to adjust the convergence speed. The effectiveness of the proposed fault detection method is verified using collecting data from a case of propeller entanglement, and it is compared and validated with the support vector machine with better real-time computing performance. The results indicate that in ensuring the accuracy of fault detection, the proposed electrical current and velocity information method can extract the multi-sensor cross-correlation information of the submerged propeller with lower computational burden.

Keywords: Entanglement detection, correlation analysis, variable sliding window, adjustable gain fuzzy clustering, Support Vector Machine (SVM).

1. INTRODUCTION

The entanglement fault detection of Unmanned Surface Vehicle (USV) propeller has evolved from a single sensor signal diagnosis method to a multi sensor signal diagnosis method. In current research on USV propeller entanglement diagnosis, most fault detection models are based on fault identification using signals collected by a single sensor. However, for complex USV propulsion systems, the fault feature information contained in a single sensor signal is limited, and the diagnostic performance of the model is greatly affected by the presence of ocean noise interference factors such as random ocean currents (Liu et al., 2020; Liu et al., 2022). Therefore, it is necessary to develop a fault diagnosis method for USV propeller based on multi-sensor signal fusion to suppress noise in fault signals and obtain sufficient and complementary feature information, in order to improve the certainty and the stability of fault detection results. The fault detection methods include the State Observer (Wang et al., 2023; Zhao et al., 2022), Wavelet Analysis (Li et al., 2012), Support Vector Machine (SVM) (Yang et al., 2016), Hidden Markov Model (Cao et al., 2018; Liu et al., 2016), and Neural Network (Xu et al., 2024; Zhu et al., 2022), and so on. Deep Neural Networks (DNN)can perform end-to-end diagnosis, effectively overcoming the drawbacks of independent feature extraction and fault classification in traditional fault diagnosis processes, and is not limited by the specific architecture of USV. It has good generalization ability and is currently the mainstream method. The advancement of artificial intelligence technology has led scholars both domestically and internationally to propose numerous enhanced Deep Neural Network (DNN) models. Currently, the most recognized DNN models include convolutional neural networks (Tsai et al., 2021), autoencoders (Jiang et al., 2021), and recurrent neural networks (Ji et al., 2021; Ni et al., 2021; Xu et al.,2022). Although deep neural networks demonstrate strong capabilities in extracting features and have achieved considerable success in diagnosing faults in USV propellers, the current methods for detecting propeller faults in USVs using deep neural networks encounter a limitation.

Specifically, these methods demand a substantial volume of samples to effectively train the model parameters. However, in practical situations, collecting sufficient data samples for each USV propeller fault category may be unsafe and time-consuming. How to use limited training sample data to achieve accurate diagnosis of USV propellers will be a challenge. The data-driven diagnostic method, often referred to as the model-free diagnostic approach, eliminates the need for constructing a precise system dynamic model and doesn't delve into the intricate structure and dynamic mechanisms of the USV. Instead, it relies on analyzing the state data of the USV to determine the fault type of the propeller, thereby enabling efficient fault diagnosis (Ni et al., 2003; Long et al., 2021).

Fig. 1. USV in the sea with Enteromorpha.

Fig. 1. shows the USV sailing to the target point distributed with Enteromorpha prolifera.When the propeller of USV becomes entangled, it produces an abnormal sound, the propeller's electrical current increases instantaneously, and its velocity decreases sharply (Yuan et al., 2021). This entanglement fault is distinguishable from when the propeller velocity is adjusted, as in that case, the current and propeller velocity increases simultaneously. If the entanglement persists, both the electrical current and velocity information are likely to exhibit a relatively stable pattern over a specific duration. Furthermore, these sampled signals are intertwined not only in their physical proximity during equipment operation but also temporally, indicating a connection that endures over time. Fault-detection systems and model-based diagnostics have been developed to identify equipment failures. However, the capabilities of the underlying model determine their effectiveness in abstracting from the robot's physical reality. The cross-correlation between parameters provides valuable information about equipment health, including the status and type of fault. Our research presents a model-free approach to detecting entanglement fault of submerged propellers using sensors data. The paper proposes an entanglement detection method that combines current and rotational propeller velocity information correlation analysis with adjustable gain fuzzy clustering. This method addresses the real-time entanglement detection problem with variable sliding sampling window in cases of entanglement. Initially, the correlation between standardized propeller velocity and electrical current signals is computed within a sliding window. Subsequently, both the across-correlation and autocorrelation matrices are constructed. Following this, a functional sliding window comprising data-collecting series is employed to assess the temporal variation in correlation coefficients between electrical current and velocity information. The paper is structured as follows:

Section 1: The development status and research methods of propeller fault diagnosis are introduced, and the main idea of this paper is also introduced.

Section 2: It involves fault detection of current and rotation speed coordinate analysis. The fault detection flow is introduced, and the signal correlation matrix-based adjustable gain fuzzy clustering is proposed. Then, it is involved that the adjustable gain clustering algorithm. And a kind of SVM-based single sensor fault detection flowing is also introduced to compare with the fault detection method proposed in this paper.

Section 3: In this section, the details on the signal acquisition method for the propeller entanglement fault sensor is depicted.And the implementation details of the proposed algorithm for entanglement detection is carried out based on cross-correlation analysis of electrical current and velocity information. Finally, it refers to the presentation and analysis of the results obtained from the entanglement detection process.

Section 4: Summarization and concluding remarks.

2. FAULT DETECTION OF CURRENT AND ROTATION SPEED COORDINATE ANALYSIS

The submerged propeller is equipped with a propeller current and speed measurement instrument (see Fig.1). The current of the propeller motor is measured through a Hall current sensor, and the speed of the propeller is measured through an encoder. The CAN bus protocol is used between the lower main control board and the propeller to exchange information with the propeller, sends the speed control command from user to the thruster, collects the output values of the current sensor and the speed sensor, and packages the collected sensor data and further transmits it to the shore station data center in real time through the wireless bridge. The data center parses the protocol data transmitted from the USV, analyzes the protocol data of current and speed fields, displays them through the upper computer data center software, and stores the parsed data in the database. It can be exported to an Excel table for subsequent algorithm processing. In July 2022, USV fault diagnosis test was conducted in the Tuandao Bay, Qingdao.

Fig. 2. The submerged propeller of USV.

As a single current or speed sensor is used for fault diagnosis, it is impossible to correctly distinguish whether it is the normal control speed regulation operation of the operator or the current and voltage fluctuations caused by the fault. To tackle the limitation of single measurement sensors that do not fully leverage the entanglement fault information from submerged propellers, the correlation matrix of electrical current and velocity information is used to carry out a feature extraction method. The correlation characteristics of electrical current and velocity information are adopted, enabling comprehensive utilization of cross-correlation even in the presence of propeller entanglement. A kind of adjustable gain fuzzy clustering algorithm with fuzzy logic improvement is proposed to employ membership values to assess the extent to which each data point belongs to a specific cluster. Therefore, in order to detect effectively the entanglement of the submerged 34nálisis, the following steps are designed:

Step 1: Initialization of Parameters: Initiate parameters such as the sliding window size, correlation threshold, sampling number, and others.

Step 2: Data Collection: Acquire electrical current and velocity data within the predefined sliding window.

Step 3: Standardization: Standardize the electrical current and velocity data for each sliding window.

Step 4: Cross-correlation Calculation: Compute the cross-correlation coefficient for each sliding window between the normalized electrical current and velocity information.

Step 5: Correlation Matrix Formation: Organize the calculated correlation coefficients into a correlation matrix.

Step 6: Entanglement Fault Detection: Utilize the proposed fuzzy clustering method for the detection of entanglement fault, employing a predetermined threshold parameter.

Step 7: Slide to next sampling window with given window length.

The entanglement detection process for submerged propellers relies on the correlation 34nálisis of electrical current and velocity information, employing the proposed algorithm within each sliding window, as illustrated in Fig. 3.

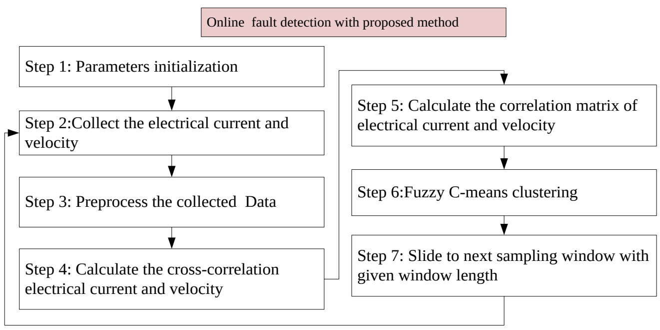

Fig. 3. Online fault detection with proposed method.

2.1 Variable Sliding Window based Correction Matrix

The subsequent explanation outlines the process for calculating the correlation matrix in the feature extraction method for both electrical current and velocity information. The electrical current and velocity information of the submerged propeller under normal control and entanglement conditions are captured through electrical current and velocity sensors. The collected data within a data-collecting window are then standardized using the following equation

$$\hat{x}_i^j(t) = \frac{x_i^j(t) - x_i^{ave}(t)}{x_i^{\max}(t) - x_i^{\min}(t)}, i = 1, 2 \ ; \ j = 1, \cdots, n(t) \tag{1}$$

where $i = 1$ denotes the current senor, and $i = 2$ denotes the rotation speed sensor. And $x_i^j(t)$ denotes the jth value of the ith sensor at time t and $\hat{x}_i^j(t)$ denotes the normalized jth value in the ith sensor at sampling time t; $x_i^{ave}(t)$ denotes the average value of collected data of the ith sensor within the given sliding sampling window, $x_i^{ave}(t) = \sum_{j=1}^{n} x_i^j(t) \big/ n(t)$; $x_i^{\min}(t)$ denotes the minimum one of the sampled ith sensor data in the given sliding window; $x_i^{\max}(t)$ is the maximum value of the ith sensor in the sliding window; $n(t)$ is the number of data-collecting points. The jth sensor's collecting value at t time is denoted by $x_i^j(t)$, meanwhile the unalized value is denoted by $\hat{x}_i^j(t)$. The current sliding window's average, minimum, and maximum values are represented by $x_i^{ave}(t)$, $x_i^{\min}(t)$, and $x_i^{\max}(t)$, where $x_i^{ave}(t) = \sum_{j=1}^{n} x_i^j(t) \big/ n(t)$, respectively. The number of data-collecting points in a sliding window at time t is represented by $n(t)$.

The normalized across-correlation coefficient of the velocity and electrical current information sensor signals at sampling time t is denoted by $\rho_{ii'}(t, n(t))$,

$$\rho_{ii'}(t, n(t)) = \frac{Cov(\hat{x}_i(t), \hat{x}_{i'}(t))}{\sigma_{\hat{x}_i}(t)\sigma_{\hat{x}_{i'}}(t)} = \frac{\sum_{j=1}^{n} \frac{(\hat{x}_i^j(t) - \hat{x}_i^{ave}(t))}{\sigma_{\hat{x}_i}(t)} \frac{(\hat{x}_{i'}^j(t) - \hat{x}_{i'}^{ave}(t))}{\sigma_{\hat{x}_{i'}}(t)}}{n(t)}, \tag{2}$$

where

$$\sigma_{\hat{x}_i}(t) = \sqrt{\frac{\sum_{j=1}^{n} (\hat{x}_i^j(t) - \hat{x}_i^{ave}(t))^2}{n(t)}}, \tag{3}$$

$$\sigma_{\hat{x}_{i'}}(t) = \sqrt{\frac{\sum_{j=1}^{n} (\hat{x}_{i'}^j(t) - \hat{x}_{i'}^{ave}(t))^2}{n(t)}}, \tag{4}$$

The autocorrelation coefficient $\rho_{ii}(t, n(t))$ of the electrical current or the velocity information with normalization at sampling time t is

$$\rho_{ii}(t, n(t)) = \frac{Cov(\hat{x}_i(t), \hat{x}_i(t - T_w))}{\sigma_{\hat{x}_i}(t)\sigma_{\hat{x}_i}(t - T_w)} = \frac{\sum_{j=1}^{n} \frac{(\hat{x}_i^j(t) - \hat{x}_i^{ave}(t))}{\sigma_{\hat{x}_i}(t)} \frac{(\hat{x}_i^j(t - T_w) - \hat{x}_i^{ave}(t - T_w))}{\sigma_{\hat{x}_i}(t - T_w)}}{n(t)}, \tag{5}$$

where

$$\sigma_{\hat{x}_i}(t)=\sqrt{\frac{\sum_{j=1}^{n}(\hat{x}_i^j(t)-\hat{x}_i^{ave}(t))^2}{n(t)}}, \tag{6}$$

$$\sigma_{\hat{x}_i}(t-T_w)=\sqrt{\frac{\sum_{j=1}^{n}(\hat{x}_i^j(t-T_w)-\hat{x}_i^{ave}(t-T_w))^2}{n(t)}}, \tag{7}$$

The sliding window T_w is used to capture accurately the change of correlation coefficient curve for distinguishing between entanglement and normal velocity control. Data-collecting points with low autocorrelation indicate that the velocity control has been carried out or that a propeller entanglement abnormality has occurred. To achieve this, use the sliding window technology to focus on these data-collecting points with low autocorrelation. The correlation degree matrix $\boldsymbol{R}(t,n(t))$ is constructed from cross-correlation coefficients between the sensor signals of velocity and electrical current information. The placement of each element in the matrix is defined by one of the sensor signals, with the cross-correlation coefficients involving the other sensor arranged either in a row or a column. This matrix serves as a valuable source of information regarding the correlation degree between the two sensor signals

$$\boldsymbol{R}(t,n(t))=\begin{bmatrix}\rho_{11}(t,n(t)) & \rho_{12}(t,n(t))\\ \rho_{21}(t,n(t)) & \rho_{22}(t,n(t))\end{bmatrix} \tag{8}$$

In the matrix, the elements $\rho_{ii'}(t,n(t))$ and $\rho_{ii}(t,n(t))$ signify the cross-correlation coefficient between the velocity and electrical current information. The correlation matrix $\boldsymbol{R}(t,n(t))$ of the electrical current and velocity information at a given and sampling time, denoted as t, is also provided, considering the presence of two sensor signals. The coefficients of the correlation matrix, expressed as $\boldsymbol{R}(t,n(t))$ signify the cross-correlation between the electrical current and velocity information. Examining this matrix enables the identification of potential relationships between the electrical current and velocity information of the propeller under various states, incorporating additional feature information. The correlation matrix feature extraction method facilitates the extraction of more profound features, overcoming the limitations of single entanglement detection methods that face challenges in enhancing accuracy due to insufficient feature extraction.

2.2 Adjustable Gain Clustering Algorithm

The adjustable gain fuzzy clustering algorithm with fuzzy logic improvement represents an enhancement of the traditional hard clustering method. It employs membership values to assess the extent to which each data point belongs to a specific cluster. The algorithm divides n vectors x_i ($i=1,\ldots,n$)into C groups and computes the clustering center for each group in order to minimize the non-similarity indicators function. The clustering with fuzzy logic and hard clustering vary in their strategies for grouping data points. The membership matrix, denoted as U , reflects this characteristic, where its elements range from 0 to 1, and the sum of membership degrees for the dataset equals 1. The adjustable gain fuzzy clustering involves the use of fuzzy division, allowing each point to determine its degree of belonging to each group with 0~1 membership values.

$$\sum_{i=1}^{c}u_{ij}=1,\forall j=1,\ldots,n \tag{9}$$

The cost function of adjustable gain fuzzy clustering serves as the objective function

$$J(U)=\sum_{i=1}^{c}J_i=\sum_{i=1}^{c}\sum_{j}^{n}u_{ij}^{m\cdot d_{ij}}d_{ij}^2 \tag{10}$$

The degree of belonging to each group of the ith fuzzy group data, represented by u_{ij} , locates between 0 and 1. And $m\in[2,\infty)$ denotes a weighted index. One kind of given distance description between the center $\boldsymbol{\rho}_i$ of the ith cluster and the collected data point $\boldsymbol{\rho}_i=[\rho_{ii'}\ \rho_{ii}]$ is defined as

$$d_{ij}=\frac{\sum_{i=1,j=1}^{i=c,j=n}|\boldsymbol{\rho}_i||\boldsymbol{\rho}_j|}{\sqrt{\sum_{i=1}^{c}|\boldsymbol{\rho}_i|^2}\sqrt{\sum_{j=1}^{n}|\boldsymbol{\rho}_j|^2}}.$$

The cost function can be constructed to determine the minimum value of Equation (10):

$$\begin{aligned}\bar{J}(U,\lambda_1,\ldots,\lambda_n)&=J(U)+\sum_{j=1}^{n}\lambda_j(\sum_{i=1}^{c}u_{ij}-1)\\ &=\sum_{i=1}^{c}\sum_{j}^{n}u_{ij}^{m}d_{ij}^2+\sum_{j=1}^{n}\lambda_j(\sum_{i=1}^{c}u_{ij}-1)\end{aligned} \tag{11}$$

The n Lagrange multipliers of Equation (11) represent the constraint by $\lambda_j(j=1,\ldots,n)$. Derive all input parameters and necessary conditions to minimize Equation (10).

$$\boldsymbol{\rho}_i=\frac{\sum_{j=1}^{n}u_{ij}^{m}\boldsymbol{\rho}_j}{\sum_{j=1}^{n}u_{ij}^{m}}, \tag{12}$$

$$u_{ij}=\frac{1}{\sum_{k=1}^{c}\left(\frac{d_{ij}}{d_{kj}}\right)^{k/(km-1)}} \tag{13}$$

where k is an adjustable gain parameter.

The adjustable gain fuzzy clustering algorithm with adjustable fuzzy parameter is an iterative process that follows these steps to capture the cluster center c_i a.nd membership matrix U . A random number between 0 and 1 is assigned to initialize the membership matrix U , that satisfies the constraint conditions in Equation (9). Next, the cluster center c_i, $i=1,\ldots,c$ is calculated using Equation (12). Then, the cost function is determined based on Equation (10). The algorithm will terminate if the cost function is less than a specified threshold or if the change in the last function value is below the threshold Finally, the updated matrix U is calculated using Equation (13) and the flow repeats from the beginning. The correlation matrix serves as the input for the proposed clustering algorithm, aiming to discern entanglement fault feature data, with algorithm parameters optimized for efficiency.

2.3 Support Vector Machine based Data Classification and Fault Detection Flow

Support Vector Machine (SVM) is extensively applied in fault diagnosis and classification decisions, employing structural risk minimization as the guiding criterion. It effectively addresses linear indivisibility in low-dimensional spaces by achieving linear separability with higher probability in higher-dimensional spaces. The fundamental idea involves identifying a hyperplane in the higher-dimensional space that maximizes the spacing between categories.

This is realized by defining a mapping function, denoted as φ, to map vectors from the low-dimensional to the higher-dimensional space, where $\varphi(\boldsymbol{x})$ represents the vector in the higher-dimensional space. The hyperplane's expression is given by

$$\begin{cases} \min \varphi(\boldsymbol{w},\gamma_i) = \dfrac{1}{2}\|\boldsymbol{w}\|^2 + C\sum_{i=1}^{n}\gamma_i \\ s.t.\ \ y_i\left[\boldsymbol{w}^T \cdot \varphi(\boldsymbol{x}_i) + b\right] - 1 + \gamma_i \ge 0, \gamma_i \ge 0, i = 1,2,\cdots,n \end{cases} \tag{14}$$

In the expression(14), C is the penalty coefficient of the relaxation factor, $\gamma_i > 0$ is the relaxation factor, and $y_i \in \{-1,1\}$ represents the class label of the ith sample value.

If a function is designed to be entirely consistent with the original objective function within the feasible region, and assumes very large or infinite values outside this region, then the optimization problem for the unconstrained objective function becomes equivalent to the optimization objective function with primary constraints. The Lagrange method can be employed to convert the constrained optimization problem into an unconstrained one. Leveraging the duality of Lagrange, the optimization problem (Equation 14) can be transformed into a more easily solvable unconstrained optimization problem.

Fault detection flow of current and velocity with SVM

$$\varphi(\boldsymbol{w},b,\boldsymbol{\alpha}) = \frac{1}{2}\|\boldsymbol{w}\|^2 + \lambda\sum_{i=1}^{n}\gamma_i - \sum_{i=1}^{n}\alpha_i(y_i(\boldsymbol{w}^T \cdot \varphi(\boldsymbol{x}_i) + b) - 1 + \gamma_i) \tag{15}$$

in which λ is the Lagrange multiplier. The ultimate optimal classification decision function for the sample is obtained through continuous optimization.

The kernel function is a mathematical function used to measure the similarity between two variables. In the case that the low dimensional space is linearly indivisible, through kernel calculation, push the two variables to the high dimensional space, and study the similarity between them.

Let

$$g(\boldsymbol{x}) = \text{sign}\left(\sum_{i=1}^{n}\alpha_i^* y_i \kappa(\boldsymbol{x}_i, \boldsymbol{x}_j) + b\right) \tag{16}$$

where $\kappa(\boldsymbol{x}_i, \boldsymbol{x}_j)$ represents the kernel function, and $\text{sign}()$ represents the sign function. Due to its superior processing capability and excellent adaptability to nonlinear data in comparison to other kernel functions, the Radial Basis Function (RBF) kernel performs inner product calculations in low-dimensional space, achieving a similar effect as in high-dimensional space. This is expressed as

$$\kappa(\boldsymbol{x}_i, \boldsymbol{x}_j) = e^{(-\varsigma\|x_i - x_j\|^2)}, \quad i, j = 1,\cdots,n; \varsigma > 0 \tag{17}$$

where $\boldsymbol{x}_i$ and $\boldsymbol{x}_j$ represent the ith and jth vectors, respectively, and ς represents the penalty factor.

In order to compare with the fault detection flow and algorithm proposed in this paper, a fault detection method based on support vector machine is designed based on the designed flow. The historical data is used for training, and the model is generated. Further, the current and speed data collected in real time or their coefficients are input into the model, and the classified output results of the model are obtained, respectively. The fault detection flow with SVM is as shown in Two fault detection methods based on SVM have been designed. The first is a fault detection method based on both current and velocity, utilizing collected current and velocity signals for detection. After normalization, it is trained using labeled training sets, and the accuracy of fault detection is tested using collected unlabeled signals. Fig. 4 shows the fault detection flow of current and velocity with SVM. The second method is a composite fault detection approach based on both current and velocity. After normalizing the collected current and velocity signals, they are input into SVM for training and detection. Fig.5 shows the fault detection flow with coefficients detection of current and velocity.

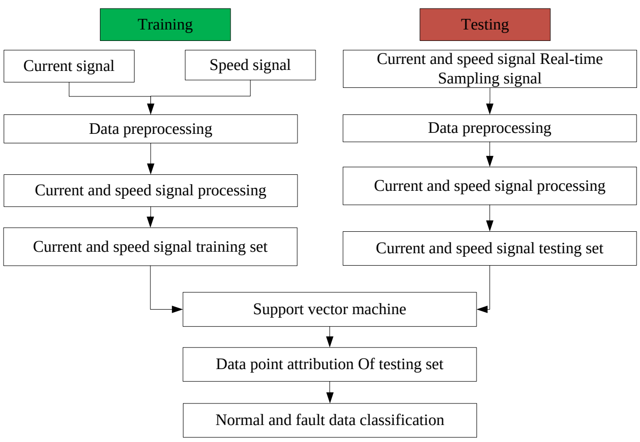

Fig. 4. SVM based Fault detection with current and velocity signals.

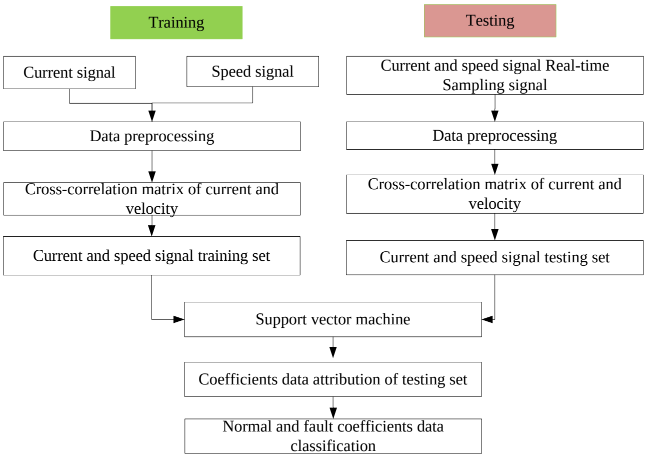

Fig. 5. SVM-based Fault detection with coefficients detection of current and velocity.

3. TESTING AND VERIFICATION

3.1 Signal Acquisition

This section details the verification process for propeller entanglement detection using the proposed method. The effectiveness of the method is validated through an experiment involving the collection of sensor data during both normal propeller operation and entanglement scenarios. A shore experiment on propeller entanglement with Enteromorpha was conducted in 2022, as depicted in Fig. 6.

We set waypoints for the USV where Enteromorpha prolifera is distributed. The USV speed is set to a constant speed. After the USV passes through Enteromorpha prolifera, the upper computer monitors that the motor current increases and fluctuates instantaneously. The roar of the propeller can be heard on the barge, and the speed is correspondingly low. However, due to the control, the speed is in a fluctuating state. Then we started the manual control function and made the thruster to reverse, thus stripping the tangled Enteromorpha prolifera.

Fig. 6. Shore experiment: propeller entanglement with Enteromorpha in 2022.

To facilitate data collection, a dedicated data-collecting software was developed, showcased in Fig. 7. The software operates at a sampling frequency of 10Hz, capturing electrical current and velocity information from the propeller under both normal and entanglement conditions. The collected current and speed data are transmitted to the shore data center through the wireless bridge and displayed through the upper computer software. The red box shows the current and speed data curve in case of fault.

The data-collecting system comprises an upper computer, a lower controller, two submerged propellers, and sensors in the instrument compartment responsible for voltage, electrical current, and velocity measurements. The upper computer's data acquisition software was created using Visual Studio 2010 C#, and the corresponding database table was established using SQL Server 2005. Fig. 5 illustrates the user interface of the acquisition software. The lower controller, employing the STM32F103 chipset, generates a PWM signal connected to the electrical controller via a watertight cable. The electrical current and velocity controller is equipped with a DC motor governor, generating a three-phase PWM signals to govern the motor rotation of the submerged propeller.

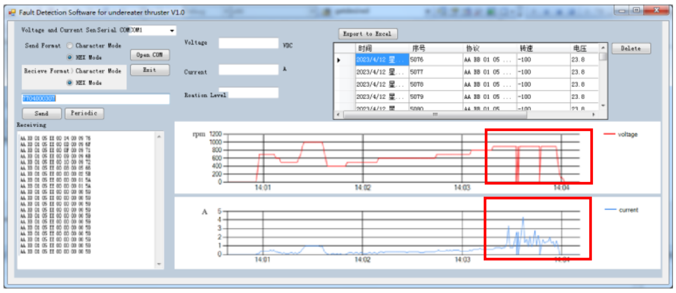

Fig. 7. Electrical current and velocity information collected by the collecting software.

In Fig. 8 and Fig. 9, the waveforms during entanglement conditions are depicted. In the red mark box are the current and speed data curves in case of fault. In both figures, the blue mark box shows the curve of current and speed change during normal speed regulation. The fluctuation of the normal data curve is caused by the manual speed control of the USV. The fluctuation of the fault curve is caused by the winding torque change of Enteromorpha prolifera on the propeller main shaft.Despite the similarity in time domain waveforms of electrical current and velocity information in both normal and entangled states, distinctions in signal amplitude are evident. However, relying solely on time domain waveform analysis makes it challenging to conclusively determine the occurrence of an entanglement fault. Table 1 shows the propeller sampling data for SVM, 500 training samples and testing ones are adopted for training and testing SVM. The proposed method is on-line runing which does not need the training and tesing data, and the initial sliding window is $T_w = 10$, and the initial step sliding window is 10. And the label is marked wiht one as Normal and zero as entangement fault for training the SVM.

Table 1. Propeller sampling data for SVM.

Signal status	**Training samples**	**Testing samples**	**Label**
Normal current signal	300	300	0
Normal velocity signal	300	300	0
Current signal with propeller entanglement	200	200	1
Velocity signal with propeller entanglement	200	200	1

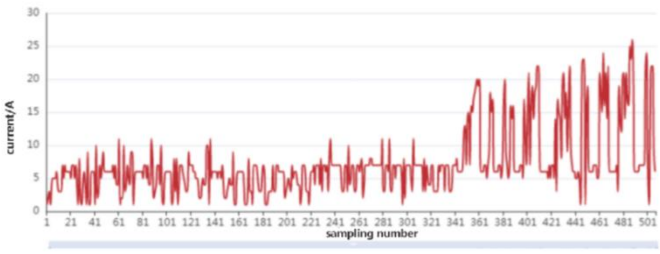

Fig. 8. The signal waveform of normal and fault current.

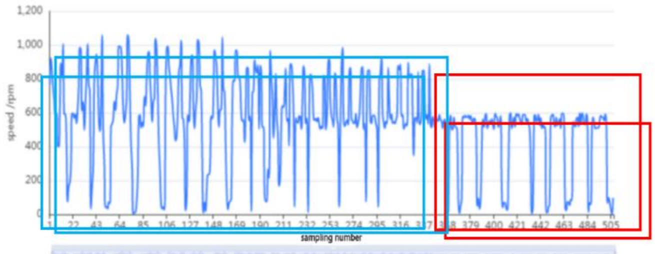

Fig. 9. The signal waveform of normal and fault velocity.

3.2 Entanglement Detection and Analysis

In this section, the data analysis and entanglement detection are carried out using the correlation matrix method. The figures below provide a visual representation of the cross-correlation between electrical current and velocity information. Darker colors indicate a stronger positive correlation, while lighter colors signify a stronger negative correlation.

Under normal propeller regulation control, as the rotational velocity of the propeller increases, there is a corresponding rise in propeller current, establishing a positive cross-correlation between electrical current and velocity information. Conversely, in the presence of an entanglement fault, the propeller velocity experiences a decrease and some fluctuations, while the propeller current exhibits an increase in the opposite direction.

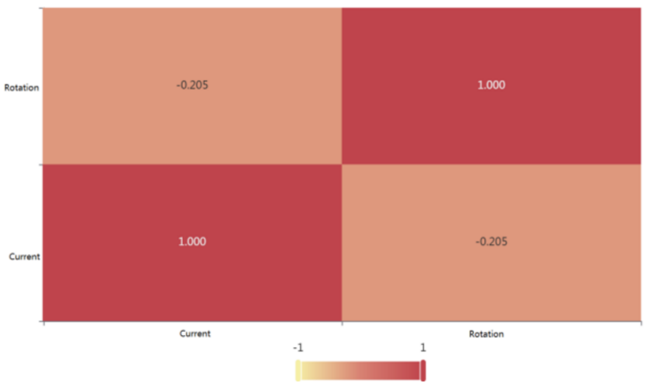

Fig. 10. The cross-correlation in entanglement condition.

Fig. 10 vividly illustrates a distinct reverse cross-correlation between electrical current and velocity information, emphasizing effective feature extraction. Fig. 11 offers insights into the cross-correlation coefficient between electrical current and velocity over time within a sliding window. Notably, it indicates a decrease in cross-correlation as entanglement occurs while the autocorrelation changes slowly. This reduction is attributed to the inclusion of more entanglement fault data as the sliding window progresses.

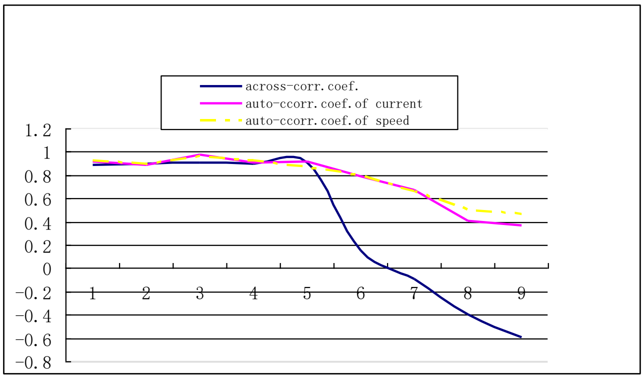

Fig. 11. The across-correlation and autocorrelation coefficient curve with sampling numbers.

3.3 Results

A confusion matrix is a table used in machine learning to evaluate the performance of a classification algorithm. It displays the number of true positive (TP), true negative (TN), false positive (FP), and false negative (FN) predictions made by the model. Fig. 12 and Fig. 13 display the confusion matrix diagrams for different methods. Fig. 12 shows the matrix diagram with the proposed method based on correlation analysis. The diagonal line represents correct predictions, while errors are shown outside the diagonal. The yellow color in the diagram indicates a large number, while black indicates a small value. The results indicate that using current and velocity signals without correction matrix for entanglement detection yields a low detection rate.

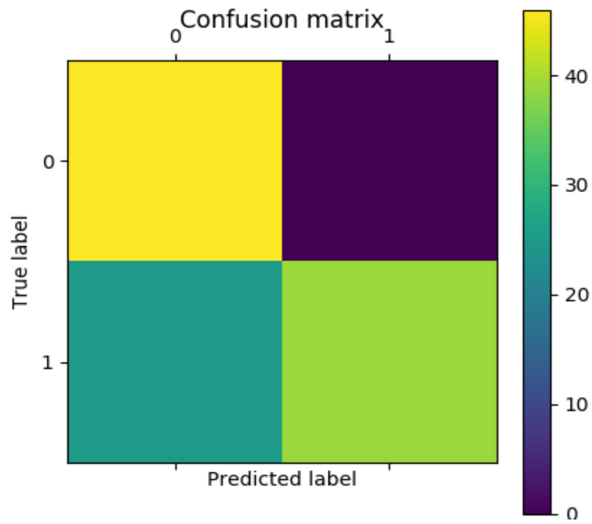

Fig. 12. The confusion matrix diagram with current and velocity coefficients.

Fig. 14 displays the SVM when $C = 10$ classification results for the current and spped sensors signal. The x-axis represents the standardized velocity signal, and the y-axis illustrates the standardized current signal. In Fig. 15, the application of SVM is demonstrated for coefficients classification using $C = 10$. The x-axis represents the autocorrelation coefficient, and the y-axis illustrates the cross-correlation coefficient. The data points with green color correspond to normal correlation coefficients, whereas the data points with red color signify correlation coefficients associated with entanglement.

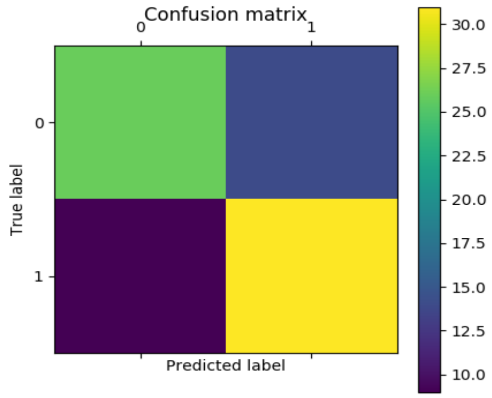

Fig. 13. The confusion matrix diagram with the proposed method.

Fig. 16 displays the results of the correlation classification with proposed method. The proposed algorithm parameters include an initial number of data-collecting points for each data-collecting group $n(0)=60$ and an initial sliding window $T_w=10$ of approximately 1 second interval, the weighted index $m=3$ of the adjustable gain fuzzy clustering coefficient, the adjustable gain parameter $k=2$. If the autocorrelation of the sample is below the correlation threshold $\rho_{ii}^{threshold}=0.9$, the number of data-collecting points will change to $n(t)=30$ and the sliding window will change to $T_w=5$. The clustering $c=2$ will be performed, using a weighted index $m=3$ of and a penalty factor $\xi=10$ in the support vector machine. The analysis of the detection results,as shown in Table 2, shows that the single current detection yields a detection accuracy rate 65.1%, the single speed detection yields a detection accuracy rate 52.8%; using the current and velocity signals yields a detection accuracy rate of 85.7%, the proposed method based on correlation analysis yields a detection rate of 96.3%, while using the coefficients of current and velocity yield a detection rate of 97.9%.

Table 2. Fault Detection Results.

Detection methods	Accuracy
The single current detection	65.1%
The single speed detection	52.8%
The composite current and velocity detection with SVM	85.7%
The coefficients detection of current and velocity	97.9%
The proposed method based on correlation analysis	96.3%

The proposed method based on correlation analysis detection rate is higher than the one in 85.7% for composite current and velocity detection method with SVM, but the detection rate is lower than the one in 97.9% of coefficients detection mehtod for current and velocity with optimal parameters.

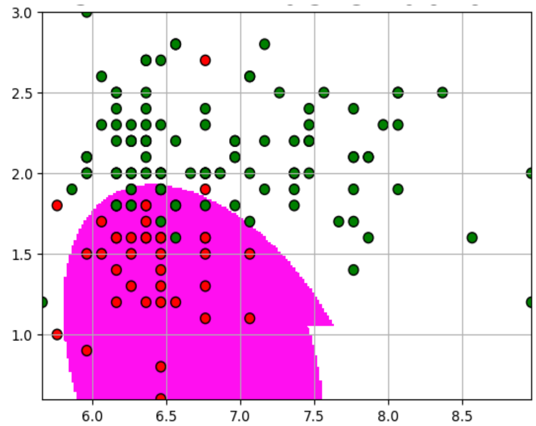

Fig. 14. The detection result with composite current and velocity signals and SVM.

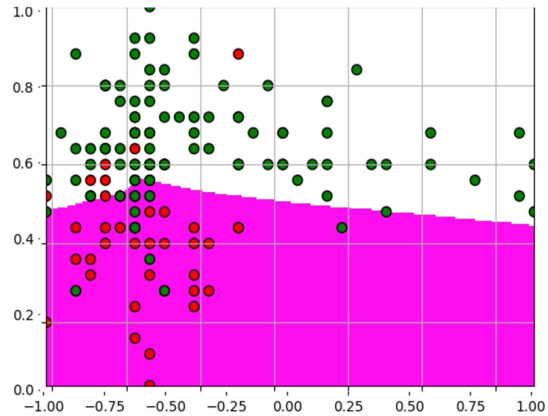

Fig. 15. The detection resulst with current and velocity coefficients and SVM.

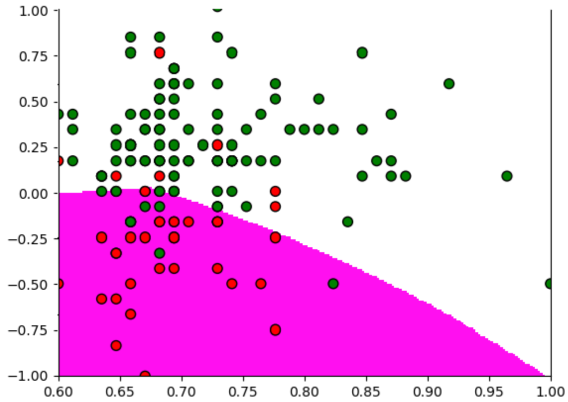

Fig. 16. The detection resulst with the proposed method

Nevertheless, the algorithm proposed attains an entanglement detection accuracy rate of 96.3%, a substantial improvement over the detection rate using the composite current and velocity detection method with SVM for entanglement detection, because it can not it yields a suboptimal entanglement fault detection rate and inadequate fault extraction.

When using a single current sensor for fault detection, this method cannot differentiate between manual speed adjustment and entanglement faults. This is because during speed adjustment, the current signal also exhibits an increasing trend, without considering the decrease in speed signal, resulting in a lower recognition accuracy. Similarly, using only the speed signal alone produces a similar effect. The composite current and voltage signals for detection can improve the accuracy of fault detection. However, the model requires a longer training time, and the trained model exhibits weaker generalization capability.However, through the consideration of cross-correlation between electrical current and velocity information, it becomes possible to extract entanglement fault features from both sensors, thereby enhancing the accuracy of entanglement detection.

4. CONCLUSIONS

This paper proposes a entanglement detection method for submerged propellers that utilizes cross-correlation analysis between electrical current and velocity information, as well as variable sliding window and adjustable gain f adjustable gain fuzzy clustering. This method can solve the issues of incomplete entanglement fault characteristics and low detection accuracy that arise when using original signal for entanglement of submerged propellers; meanwhile it id of lower computational complexity. The correlation analysis and the proposed method are verified using electrical current and velocity information from submerged propellers. To capture accurately the change of correlation coefficient curve, the variable sliding window method is adopted, which can calculate the fault occurrence time within one short interval. The outcomes demonstrate the efficacy of the proposed method in efficiently extracting cross-correlation between electrical current and velocity information during entanglement fault mode. This leads to an entanglement detection accuracy rate of 96.3%, representing a notable enhancement over the Support Vector Machine method that relies solely on electrical current and velocity information for entanglement detection. This method can online distinguish whether the entanglement fault has occurred, or not propeller velocity modulation is carried out, and analyze the changing of the correlation coefficient curve, the proposed method also can determine the occurrence of entanglement by increasing the size of data collection and reducing the size of the sliding window.

AKNOWLEDGMENTS

This work is financially supported by Shandong Teaching Reform Research Project(M2022338), Open Fund Project of Key Laboratory of Ocean Observation Technology, MNR (2021klootA10) and the Natural Science Foundation of Shandong Province (ZR2022ZD38, ZR2021MD070) .

REFERENCES

Cao L., Xia Y.B., Lin Z.L. (2018). Bearing fault diagnosis method based on GMM and Coupled Hidden Markov model Prognostics and System Health Management Conference (PHM-Chongqing), *Prognostics and System Health Management Conference*, pp.932-936.

Ji D., Yao X., Li S., et al. (2021). Model-Free Fault Diagnosis for Autonomous Underwater Vehicles Using Sequence Convolutional Neural Network. *Ocean Engineering*, 232: 108874.

Jiang Y., Feng C., He B., et al. (2021). Actuator Fault Diagnosis in Autonomous Underwater Vehicle Based on Neural Network. *Sensors and Actuators A: Physical*, 324: 112668.

Li S.E., Lv F., Fu C. (2012). Wavelet Selection in Fault Diagnosis of Wavelet Transform, *International Conference on Manufacturing Engineering and Automation*, pp.2127-2130.

Liu F., Tang H., Qin Y., Duan C., Luo J., Pu H. (2022). Review on fault diagnosis of unmanned underwater vehicles, *Ocean Engineering*, 243, 1-9.

Liu T., Chen J., Dong G.M. (2016). Identification of bearing faults using linear discriminate analysis and continuous hidden Markov model, *Proceedings of the Institution Mechanical Engineers Part C-Journal of Mechanical Engineering Science*, pp.1658-1672.

Liu X., Zhang M., Wang S. (2020). Adaptive Region Tracking Control with Prescribed Transient Performance for Autonomous Underwater Vehicle with Thruster Fault. *Ocean Engineering*, 196: 106804.

Long Z., Zhang X., Zhang L., et al. (2021). Motor Fault Diagnosis Using Attention Mechanism and Improved Ada boost Driven by Multi-Sensor Information. *Measurement*, 170: 108718.

Ni L., Fuller C.R. (2003). Control Reconfiguration Based on Hierarchical Fault Detection and Identification for Unmanned Underwater Vehicles. *Journal of Vibration and Control*, 9(7): 735-748.

Ni P. and Wen X. (2021). Fault diagnosis of satellite attitude actuator based on recurrent neural network, *Chinese Space Science and Technology*, 41 (4):121-126.

Tsai C. M., Wang C.S., Chung J., et al. (2021). Multi-Sensor Fault Diagnosis of Underwater Thruster Propeller Based on Deep Learning. *Sensors*, 21(21): 7187.

Xu X.Z, Li Z.Y., Qian W. (2024). Fault diagnosis of gas turbine generator bearings using enhanced valuable sample strategy and convolutional neural network, *Measurement Science and Technology,* 35 (1).

Xue T., Wang H.G., Liu Z.X. (2022). Diagnosis of Rolling Bearings Based on Total Vector Convolutional Recurrent Neural Networks, *8th International Conference on Mechatronics System and Robots (ICMSR)*, ICMSR, pp.15-19.

Wang B., Miao X., Wei H., Saklain M.D., et al. (2023). A novel fuzzy time series method based on Dynamic Ridge Polynomial Neural Network neural network with penalty term and Fuzzy Clustering analysis, *IEEE Access*.

Yang C.M., Hou J. (2016). Fed-batch fermentation penicillin process fault diagnosis and detection based on support vector machine, *Neurocomputing*,190:117-123.

Yuan J., Wan J.H., Zhang W.X., et al. (2021). *Journal of Robotics*, 2021, (1):1-11.

Zhao J., Zhang K., Hou M., et al. (2022). Actuator Fault Detection for Masonry Robot Manipulator Arm with the Interval Observer. *Journal of Field Robotics*,40(2): 147-160.

Zhu D.Q., Cheng X.L., Yang L., Chen Y.S., Yang S.X. (2022). Information Fusion Fault Diagnosis Method for Deep-Sea Human Occupied Vehicle Thruster Based on Deep Belief Network. *IEEE Trans. on Cybernetics*,52(9): 9414-9427.